Theoretical study of the electronic structure of KLi molecule: Adiabatic and diabatic potential energy curves and dipole moments

ARTICLE *in* CHEMICAL PHYSICS · MAY 2012

Impact Factor: 1.65 · DOI: 10.1016/j.chemphys.2011.07.010

4 AUTHORS:

Riadh Dardouri
University of Monastir
8 PUBLICATIONS **24** CITATIONS
SEE PROFILE

Héla Habli
University of Monastir
9 PUBLICATIONS **31** CITATIONS
SEE PROFILE

Brahim Oujia
University of Monastir
61 PUBLICATIONS **296** CITATIONS
SEE PROFILE

Florent Xavier Gadéa
Paul Sabatier University - Toulouse III
153 PUBLICATIONS **2,818** CITATIONS
SEE PROFILE

Chemical Physics 399 (2012) 65–79

Contents lists available at ScienceDirect

Chemical Physics

journal homepage: www.elsevier.com/locate/chemphys

Theoretical study of the electronic structure of KLi molecule: Adiabatic and diabatic potential energy curves and dipole moments

Riadh Dardouri [a,*], Héla Habli [a], Brahim Oujia [b], Florent Xavier Gadéa [b]

[a] Laboratoire de Physique Quantique, Faculté des Sciences de Monastir, Avenue de l'Environnement, 5019 Monastir, Tunisia
[b] Laboratoire de Chimie et Physique Quantique, UMR 5626 du CNRS, Université de Toulouse, UPS, 118 route de Narbonne, 31062 Toulouse Cedex 4, France

ARTICLE INFO

Article history:
Available online 20 July 2011

Keywords:
Diabatic potentials
Adiabatic potentials
Dipole moments
Ionic limit
Pseudo-potential
Correlation
Full valence *CI* approach
Spectroscopic constants
Potential energy curves

ABSTRACT

For all states dissociating below the ionic limit Li^-K^+, we perform an adiabatic and diabatic study for $^1\Sigma^+$ electronic states dissociating into K (4s, 4p, 4d, 5s, 5p, 5d, 6s) + Li (2s, 2p, 3s). Furthermore, we present the adiabatic results for the 1–11 $^3\Sigma$, 1–8 $^{1,3}\Pi$ and 1–4 $^{1,3}\Delta$ states. The present calculations on the KLi molecule are complementary to previous theoretical work on this system, including recently observed electronic states that had not been calculated previously. The calculations rely on an *ab initio* pseudo-potential, Core Polarization Potential operators for the core–valence correlation and full valence *CI* approaches, combined to an efficient diabatization procedure. For the low-lying states, our spectroscopic constants and vibrational level spacing are in good agreement with the available experimental data. Diabatic potentials and permanent dipole moments are analyzed, revealing the strong imprint of the ionic state in the $^1\Sigma^+$ adiabatic states.

1. Introduction

Cold and ultra-cold molecules have received increasing attention in recent years due to the significant advances and the potential new applications that they offer in several reactions, like ultra-high resolution molecular spectroscopy, tests of fundamental theories in physics, clocks based on molecular transitions, full control of the dynamics of cold chemical reactions, design of quantum information devices [1–4]. Among the various approaches to form stable cold molecules, the photo-association (PA) of laser-cooled atoms into an excited molecule followed by stabilization via spontaneous emission has been proven as very successful method to obtain large and dense samples of ultra-cold homo-nuclear and hetero-nuclear alkali dimers [3]. Ultra-cold molecules in the lowest vibrational level of their electronic ground state have been observed in this way [5,6], or through subsequent vibrational cooling using a pulsed laser [7–9]. Spectacular development in creation of ultra-cold molecules in their absolute ground level have also been achieved through the control of Feshbach resonances of ultra-cold colliding alkali atoms with external magnetic fields combined with the Stimulated Raman Adiabatic Passage (*STIRAP*) [10,11].

Several theoretical studies of the electronic structure of alkali dimers have been interested in studying the hetero-nuclear alkali dimers using various quantum chemistry methods to determine the potential energy curves of the ground and exited states of RbCs [12–14], NaRb and LiRb [15], NaCs, LiCs and CsK [16], KRb [17], LiK [18], NaK [19,20] and LiNa [21,22].

Several theoretical [23,18] and experimental [24–32] studies have been performed for the LiK molecule. The first theoretical study of the LiK molecule was made by Muller and Meyer [23] based on pseudo-potential and *CI* calculations. They have determined the spectroscopic constants for the ground and the lower excited state. Rousseau et al. [18] have made an *ab initio* calculation for the LiK molecule, where they determined the potential energy curves for the 58 lowest states of $^{1,3}\Sigma^+$, $^{1,3}\Pi$ and $^{1,3}\Delta$ symmetries.

Although realistic all-electron calculations are now feasible for KLi, we prefer to use pseudo-potential for the core and large basis sets for the valence and Rydberg states, which allows accurate descriptions of the highest excited states. The two electrons are then treated at the full configuration-interaction (*CISD*) level. Core-valence correlation effects are quite important. Here we used the well-established operator approach proposed by Müller et al. [33].

This paper presents the first *ab initio* calculation on highly-excited states of the potassium lithium molecule since we treat all the states dissociating below the ionic one (i.e., states dissociating to yield the K atom in one of the states K (4s, 4p, 4d, 5s, 5p, 5d, 6s).

The accuracy of the results can be estimated by a comparison with the numerous theoretical and experimental data for the lowest states. In addition to the adiabatic potential curves and dipole moments, we calculate diabatic *ab initio* ones and interpret them. Therefore a rather complete set of data is presented for the KLi

* Corresponding author.
E-mail address: dardouririad@yahoo.fr (R. Dardouri).

0301-0104/$ - see front matter © 2011 Elsevier B.V. All rights reserved.
doi:10.1016/j.chemphys.2011.07.010

molecule from the ground state to the highly excited states: almost all electronic states below the ionic limit, including also adiabatic potential curves for $^{1,3}\Sigma^+$, $^{1,3}\Pi$ and $^{1,3}\Delta$ states, permanent dipole moments and transition dipole moments, as well as the possible electronic couplings, for the corresponding diabatic states. This set of data can be further used to perform detailed spectroscopic studies including vibronic effects, radiative and non-radiative lifetimes.

This paper is organized as follows: In Section 2, we present the computational method and give numerical details. In Section 3, which is divided into two parts, we present the adiabatic potential energy curves and their spectroscopic constants for the ground and numerous excited states of $^{1,3}\Sigma^+$, $^{1,3}\Pi$ and $^{1,3}\Delta$ symmetries; the diabatic potential energy curves. Permanent and transition electric dipole moments are reported in Section 4. Finally, we summarize our work in Section 5.

2. Method

2.1. Computational details

In this study, the Li and K atoms are treated through the one-electron pseudo-potential proposed by Barthelat et al. [34,35] and employed in many previous works (see, for example, Ref. [36–39]). In addition, we take into account the core valence correlation in view of the operator formalism of Muller et al. [33]. The summation runs over all the polarizable cores with a dipole polarizabilty. The electric field f is created on a center produced by valence electrons and all other cores, modified by a cut-off function F with an l-dependent adjustable parameter according to the formulation of Foucrault et al. [40],

Table 1
l-Dependent cut-off radii (in [Bohr]) for the Li and K atoms.

L	Li	K
S	1.433	2.115
P	0.979	2.1125
d	0.600	1.983
f	0.400	2.0

Table 2
Atomic transition energies of the Li and K atoms (in [cm^{-1})].

Atom	Atomic levels	This work	Exp. [47]	ΔE
Lithium	Li(2s)	0.00	0.00	0.00
	Li(2p)	14903.66	14903.66	0.00
	Li(3s)	27269.42	27206.12	63.30
	Li(3p)	30919.71	30925.38	5.67
	Li(3d)	31283.08	31283.08	0.00
Potassium	K(4s)	0.00	0.00	0.00
	K(4p)	13,030	13,030	0.00
	K(5s)	21,021	21,027	6.00
	K(3d)	21,535	21,535	0.00
	K(5p)	24,725	24,716	9.00
	K(4d)	27,409	27,397	13.00
	K(6s)	27,453	27,451	2.00
	K(4f)	28,149	28,128	21.00

Table 3
Asymptotic energy of LiK electronic states (in cm^{-1}).

Asymptotes	Exp. [47]	This work	ΔE (cm^{-1})	Molecular states
Li(2s) + K(4s)	0.00	0.00	0.00	$^{1,3}\Sigma$
Li(2s) + K(4p)	13030.00	13030.00	0.00	$^{1,3}\Sigma$, $^{1,3}\Pi$
Li(2p) + K(4s)	14903.66	14903.66	0.00	$^{1,3}\Sigma$, $^{1,3}\Pi$
Li(2s) + K(5s)	21027.00	21033.00	6.00	$^{1,3}\Sigma$.
Li(2s) + K(3d)	21535.00	21535.00	0.00	$^{1,3}\Sigma$, $^{1,3}\Pi$, $^{1,3}\Delta$
Li(2s) + K(5p)	24716.00	24725.00	9.00	$^{1,3}\Sigma$, $^{1,3}\Pi$
Li(3s) + K(4s)	27206.12	27269.42	63.30	$^{1,3}\Sigma$.
Li(2s) + K(4d)	27397.00	27410.00	13.00	$^{1,3}\Sigma$, $^{1,3}\Pi$, $^{1,3}\Delta$
Li(2s) + K(6s)	27451.00	27453.00	2.00	$^{1,3}\Sigma$
Li(2p) + K(4p)	27933.66	27933.66	0.00	$^{1,3}\Sigma$, $^{1,3}\Pi$, $^{1,3}\Delta$
Li(2s) + K(4f)	28128.00	28149.00	21.00	$^{1,3}\Sigma$, $^{1,3}\Pi$, $^{1,3}\Delta$
Li^-K^+	30012.52	30025	12.48	

$$\vec{f}_\lambda = \sum_i \frac{\vec{r}_{i\lambda}}{r_{i\lambda}^3} F(r_{i\lambda}, \rho_\lambda) - \sum_{\lambda\lambda'} \frac{\vec{R}_{\lambda\lambda'}}{R_{\lambda\lambda'}^3} Z_\lambda \quad (1)$$

where $\vec{r}_{i\lambda}$ is a core–electron vector and $\vec{R}_{\lambda\lambda'}$ is a core–core vector. The cut-off operator $F(r_{i\lambda}, \rho_\lambda)$ is expressed, following the Foucroult formalism, by a step function defined by

$$F(r_{i\lambda}, \rho_\lambda) = (0 : r_{i\lambda} \langle \rho_\lambda \langle \rho_\lambda) \quad (2)$$

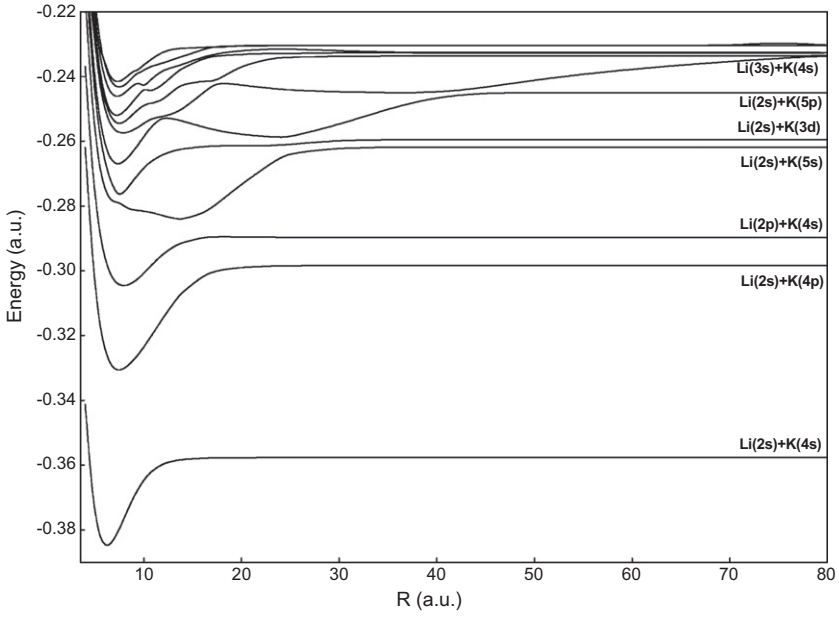

Fig. 1. Adiabatic potential energy curves for the 12 lowest $^1\Sigma^+$ states of LiK.

This has the physical meaning of excluding the valence electrons from the core region for calculating the electric field. The cut-off radius is taken to be a function of l as follows:

$$F(r_{i\lambda}, \rho_\lambda) = \sum_{l=0}^{\infty} \sum_{m=-l}^{+l} F_l(r_{i\lambda}, \rho_\lambda) |lm\lambda\rangle\langle lm\lambda| \quad (3)$$

where $[|lm\lambda\rangle\langle lm\lambda|]$ is the spherical harmonic centered on λ. In the formalism of Muller et al. [33], this cut-off function is unique for a given atom, generally adjusted to reproduce the first ionization potential. The cut-off radii given in Table 1 were optimized in order to reproduce the ionization potentials and the lowest valence s, p, and d one-electron states as deduced from the tables of atomic data. An extensive range of inter-nuclear distances has been considered ranging from 4.5 to 400 Bohr, in order to cover all the ionic-neutral crossings in the $^1\Sigma^+$ symmetry. As in LiH [41] the adiabatic and diabatic potential energy curves present various avoided crossing or crossings and undulations with repulsive barriers at short distances related to intrinsic characteristics of the Rydberg states which extend to very large inter-nuclear distance for the high states and the calculation has to extend for short to very large distances. The Gaussian type orbital basis sets on Li and K atoms, respectively, are 6s/5p/4d/2f and 8s/5p/5d/2f and the core dipole polarizability of Li^+ and K^+ respectively, are 0.1915 a_0^3 and 5.457 a_0^3.

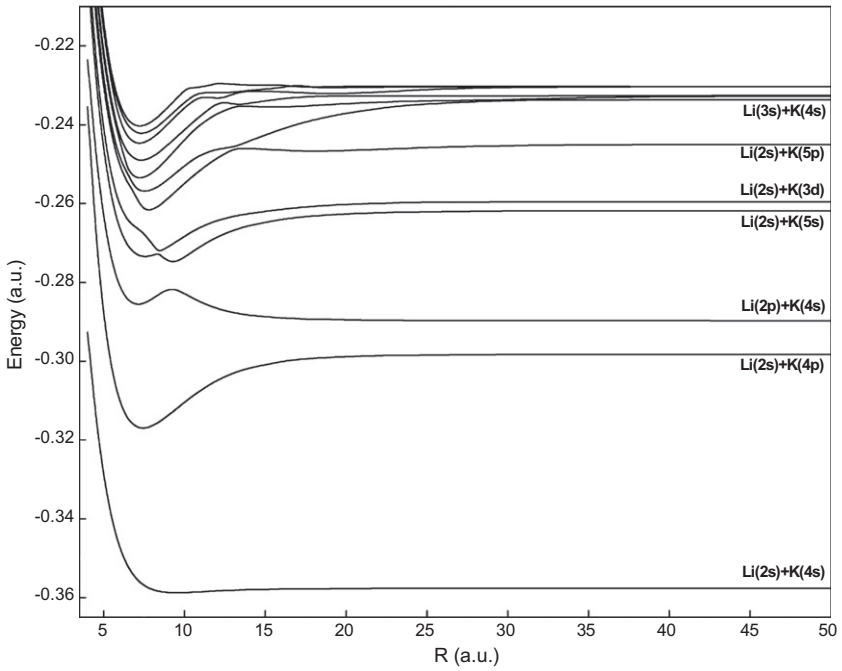

Fig. 2. Adiabatic potential energy curves for the 12 lowest $^3\Sigma^+$ states of LiK.

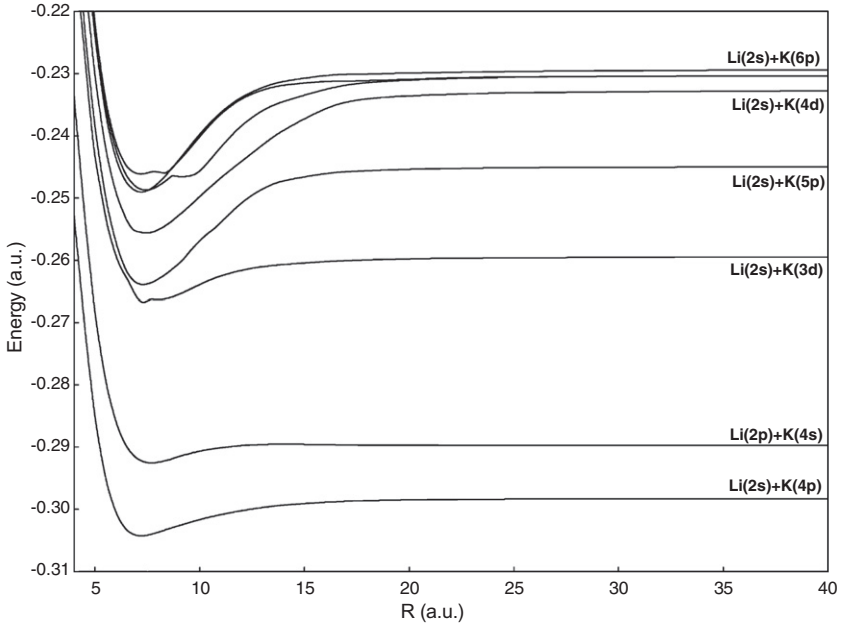

Fig. 3. Adiabatic potential energy curves for $^1\Pi$ states of LiK.

In Table 2, a comparison between our *ab initio* and the experimental work of Moore [47] energy levels for Li (2s, 2p, 3s and 3p), K (4s, 4p, 4d, 5s, 5p, 5d, 6s) atomic states are presented. Our atomic energies are in good agreement with the experimental ones. The difference between our work and the experimental values does not exceed 63 cm^{-1}. We expected such accuracy in molecular calculations.

In the present work we have considered all the potential curves for all various symmetries up to the $Li^{-}K^{+}$ dissociating limit. As can be seen in Table 3 where all dissociation limits are reported, even for this rather high in energy dissociation limit, and also for all lower ones, we get a reasonable agreement with the experimental values. The largest errors are for the (Li (3s) + K (4s)) state limit.

2.2. Diabatization

We briefly recall here the main lines of the method, more details can be found in previous publications [41,43–45]. The Born–Oppenheimer approximation is insufficient particularly in the vicinity of avoided level crossings. In these regions, the adiabatic states may be strongly coupled via non-adiabatic couplings and transitions between them may occur. These interactions are important in dynamical processes such as predissociation, inelastic or non-radiative transitions, and also in spectroscopy. Diabatic representations where the coupling is essentially electronic are thus useful. Here, we have used a method based on a crude numerical estimate of the non-adia-

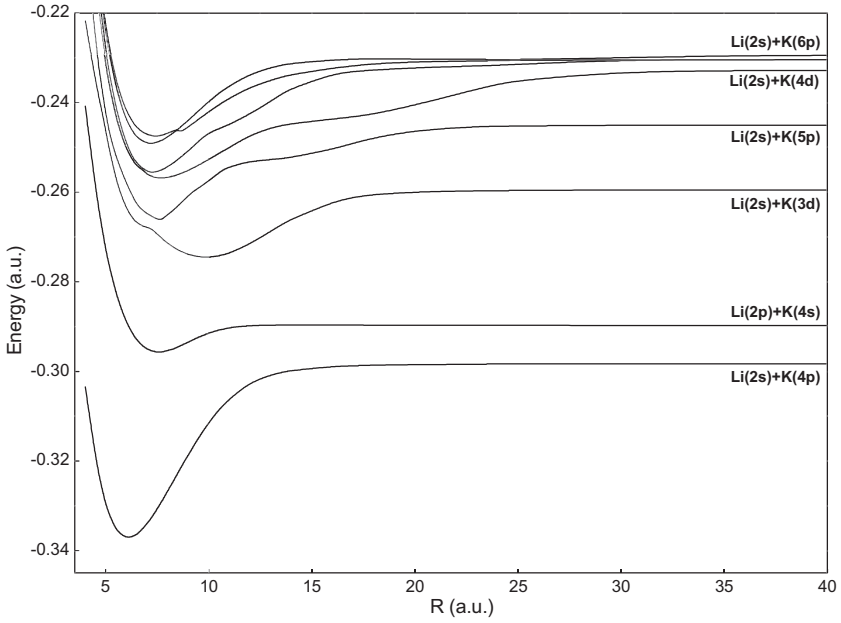

Fig. 4. Adiabatic potential energy curves for $^{3}\Pi$ states of LiK.

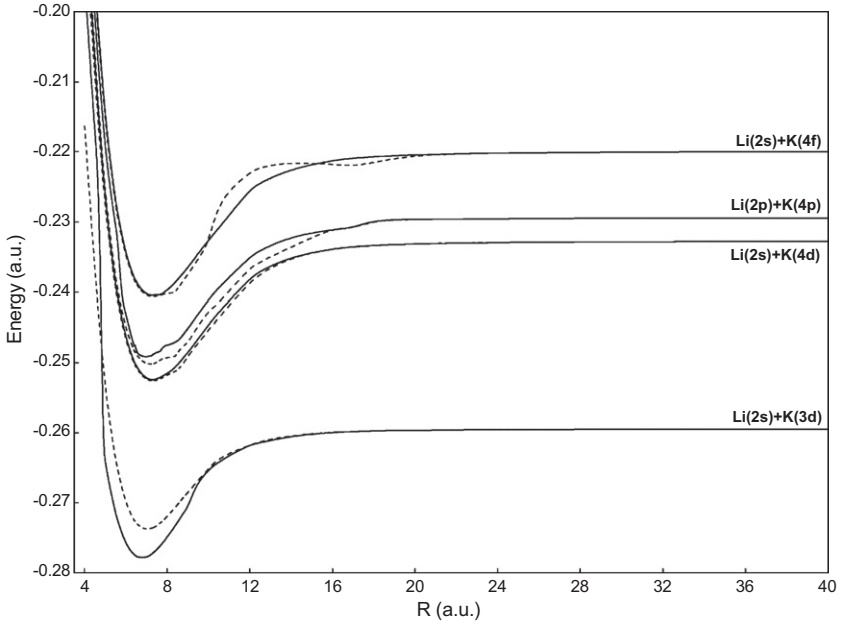

Fig. 5. Adiabatic potential energy curves for the $^{3}\Delta$ (solid lines) and the $^{1}\Delta$ (dashed lines).

Table 4
Equilibrium distance R_e (a.u.), potential well depth D_e (in cm^{-1}), vibrational constant ω_e (in cm^{-1}) and transition energy value T_e (in cm^{-1}) for the Z^+ states of LiK molecule compared with the available results in the literature.

State	R_e	D_e	ω_e	T_e	Ref.
X $^1\Sigma^+$	6.22	6197	210.75	0.00	This work
	6.24	6216	212.0386	0.00	Exp. [24]
	6.25			0.00	Exp. [25]
	6.26	6138	211.59	0.00	Theory [23]
	6.16	6220	210.90	0.00	Theory [18]
2 $^1\Sigma^+$	7.43	7167	133.74	12,798	This work
	7.362	7186	135.50	12,056	Theory [18]
3 $^1\Sigma^+$	7.91	3554	115.20	17,767	This work
	7.876	3619	115.4097	17501.178	Exp. [26]
	7.922	3618.8	115.41	17501.239	Exp. [27]
	7.76	3477	114.27	17,647	Theory [18]
4 $^1\Sigma^+$	13.97	4860	57.25	23,898	This work
	13.98				Exp. [28]
5 $^1\Sigma^+$	7.54	3680	192.35	25,600	This work
6 $^1\Sigma^+$	7.34	4801	145.30	26,794	This work
7 $^1\Sigma^+$	7.86	3578	98.50	29,061	This work
8 $^1\Sigma^+$	7.48	4565	140.96	29,631	This work
9 $^1\Sigma^+$	7.21	4208	1097.60	30,058	This work
10 $^1\Sigma^+$	7.26	2964	2724.71	31,197	This work
11 $^1\Sigma^+$	7.47	2817	1832.63	32,194	This work
12 $^1\Sigma^+$	7.30	2444	3667.35	32,337	This work

batic coupling between the adiabatic states concerned and its cancellation thanks to an appropriate unitary transformation according to effective Hamiltonian theory [42,43,45,46]. The effective Hamiltonian made use of a set of reference states, called model space, taken as adiabatic states at a very large distance, however in its alternative variational version [42]. For the crude numerical estimate of the non-adiabatic coupling, we used an effective overlap matrix between the two sets of atomic orbitals involved [44]. A choice of the common origin needs here to be done and we have set it in the atom K. This diabatization method has been shown to be very powerful for the whole series of alkali hydrides where it is the only one able to follow the ionic state from large to short distances and to exhibit its strong imprint in the adiabatic representation. The calculation is performed from the largest distance where the diabatic states are initialized to the adequate adiabatic ones, to the shorter distances, similar to an integration scheme.

However it should be emphasized that, in the alkali hydride series, the H atom presented only two states, ionic or in 1s, and therefore a rather limited basis set was used for H, without diffuse Rydberg functions, together with huge basis sets for the alkali where a large number of states where considered. Here the situation is more involved since large basis sets are used for both atoms and we are frequently on the verge of over completeness and linear dependence, particularly when involving the effective matrix connecting the two internuclear distances. Therefore the diabatization procedure used here should be considered as an attempt rather than a definitive answer.

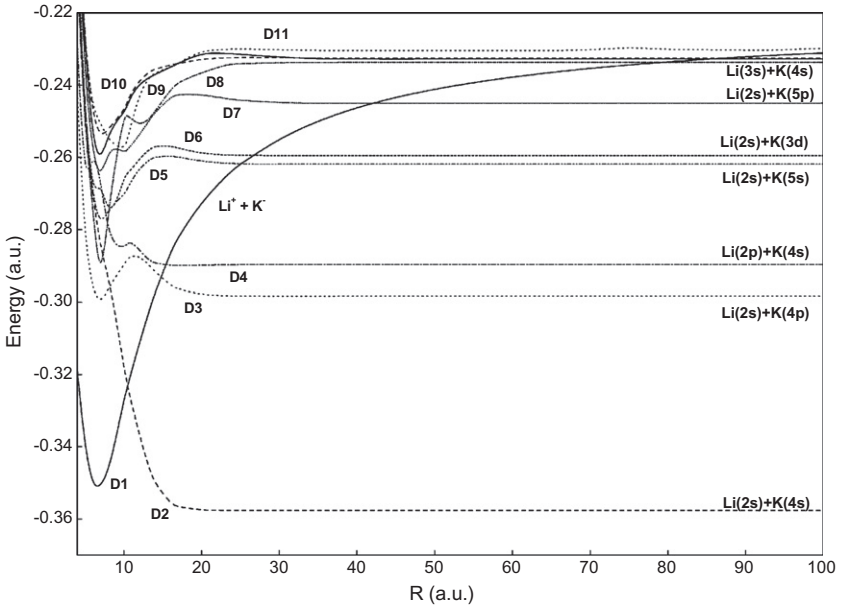

Fig. 6. Diabatic potential energy curves for the 12 lowest $^1\Sigma^+$ states of LiK.

3. Results and discussion

3.1. Adiabatic potential energy and spectroscopic constants

We have determined the adiabatic potential energy curves of 48 electronic states of $^{1,3}\Sigma^+$, $^{1,3}\Pi$, and $^{1,3}\Delta$ symmetries for the KLi molecule dissociating into K (4s, 4p, 4d, 5s, 5p, 5d, 6s) + Li (2s, 2p, 3s). The potential energy has been calculated for a large and dense grid of intermolecular distances ranging from 4.5 to 400 a.u. The $^1\Sigma^+$ and $^3\Sigma^+$ electronic states are displayed, respectively, in Figs. 1 and 2, whereas the $^{1,3}\Pi$ and $^{1,3}\Delta$ states are displayed in Figs. 3–5, respectively.

Interestingly, as can be seen in Fig. 1, the higher excited $^1\Sigma^+$ states present series of undulations, which lead to potentials with double and sometimes triple wells. Many of these particular shapes can be related to the interaction with the ionic state K^+Li^-. Some of these electronic states have been studied experimentally for the isotope $^{39}K\,^7Li$ [16,24–32]. For all these potentials, we have computed the vibrational states without rotation by solving the radial Schrödinger equation using DVR approach. The main spectroscopic constants have been determined here as the first vibrational spacing for ω_e and the vertical transition at the equilibrium distance of the ground state for T_e. These spectroscopic constants (R_e, D_e, ω_e and T_e) for the $^1\Sigma^+$ sates are presented in Table 4 and compared to the ones available in the literature. The ground state has been the most studied one, and a comparison can be done to experimental [24,25] as well as previous theoretical results [23,18]. There is a good agreement with the experimental data,

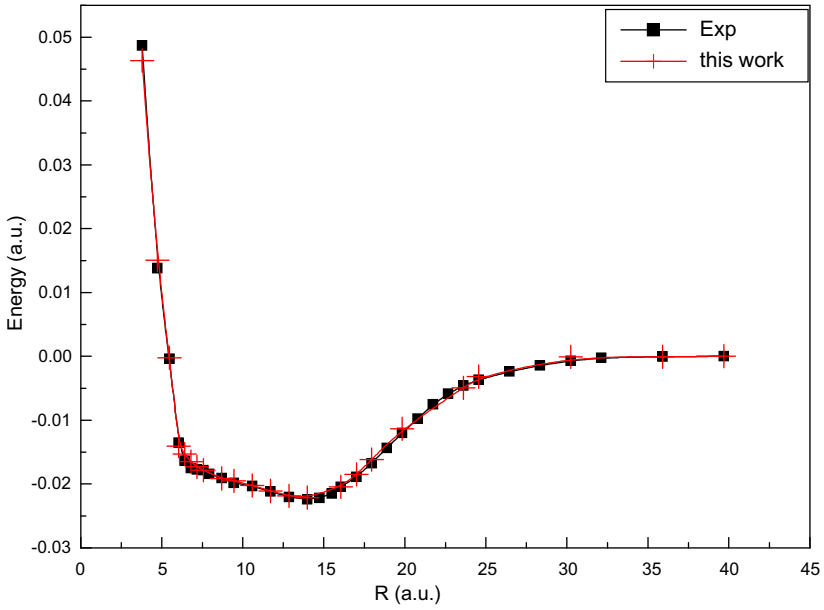

Fig. 7. Adiabatic potential energy curve for the 4 $^1\Sigma^+$ state of LiK compared with experimental result with a change of zero reference.

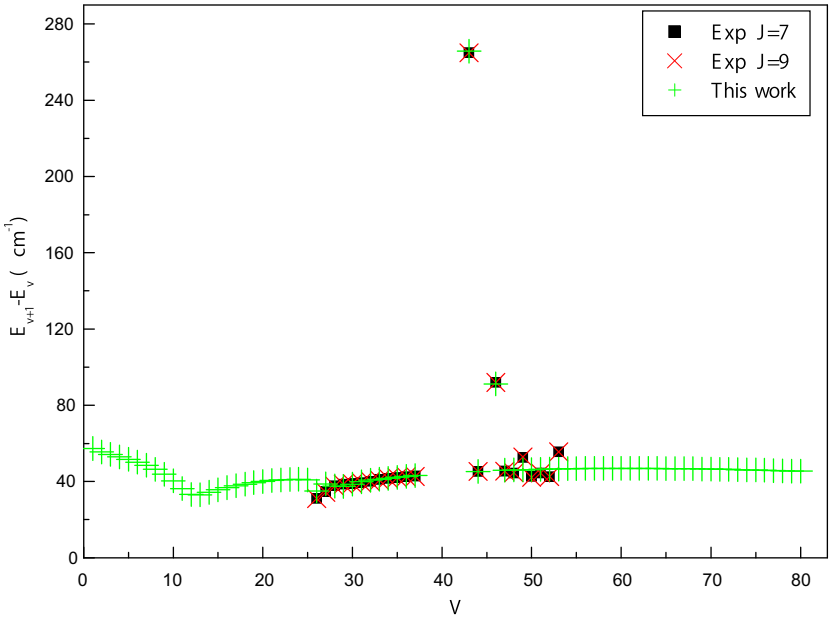

Fig. 8. Vibrational level spacings for the 4 $^1\Sigma^+$ state of the KLi compared with experimental result for $J = 7, 9$.

Table 5
Spectroscopic constants R_e (in a.u.), D_e (in cm^{-1}), ω_e (in cm^{-1}) and T_e (in cm^{-1}) for the ^3Z states of the LiK molecule compared with the available results in the literature.

State	R_e	D_e	ω_e	T_e	Ref.
$1\ ^3\Sigma^+$	9.42	276.33	37.98	5760	This work
	9.43 (±0.09)	287.0 (±4)			Exp. [29]
	9.40	273	43.97	5947	Theory [18]
$2\ ^3\Sigma^+$	7.43	4099	135.65	15,996	This work
	7.362	4309	141.89	14,931	Theory [18]
$3\ ^3\Sigma^+$	7.13	917.60		22,616	This work
$4\ ^3\Sigma^+$	7.56	2530	149.98	24,233	This work
$5\ ^3\Sigma^+$	8.45	2739	203.45	25,313	This work
$6\ ^3\Sigma^+$	7.80	3646	180.23	28,140	This work
$7\ ^3\Sigma^+$	7.53	5094	142.00	29,160	This work
$8\ ^3\Sigma^+$	7.23	4540	160.11	30,484	This work
$9\ ^3\Sigma^+$	7.32	3604	142.67	31,127	This work
$10\ ^3\Sigma^+$	7.21	3141	153.98	32,332	This work
$11\ ^3\Sigma^+$	7.34	2588	143.88	32,657	This work
$12\ ^3\Sigma^+$	7.22	2190	149.93	33,271	This work

with relative differences of about 0.2%, as well as with the previous theoretical estimations. This agreement gives confidence in the present calculation. As can be seen in Table 4, for the other states also, our results are in good agreement with the experimental data, being generally better than the previous theoretical results. This is particularly true for the second excited state, where noticeable improvement can be observed for R_e, D_e and ω_e.

The state $4\ ^1\Sigma^+$ has an unusual shape and has attracted interesting studies, mainly experimental [28]. The IPA potential has been published thanks to the observation of a large number of vibrational levels. In Fig. 7 we compare this experimentally determined potential with our *ab initio* result. The agreement is impressive, giving strong support to the present study. The vibrational spacings are reported in Fig. 8 and compared to the experimental ones. Here also the agreement is very good although we have performed calculations for $J = 0$, while experiments are for $J = 7$ and $J = 9$, therefore smooth extrapolations can be expected.

Table 5 presents the spectroscopic constants of the 1–10 $^3\Sigma^+$ states. The $1\ ^3\Sigma^+$ state has been experimentally explored recently by Salami et al. [29] it exhibits a very small potential well of 287 cm^{-1} located at an equilibrium distance of 9.38 a.u. Here also, our results are in rather good agreement with the experimental data and somewhat better than the previous theoretical ones.

The spectroscopic constants of the $^{1,3}\Pi$ and $^{1,3}\Delta$ states are presented in Tables 6 and 7. For all these states of different symmetries, many avoided crossings have been located at large internuclear distance as well as at short distance. Their existences will generate large non-adiabatic coupling and lead to an undulating behavior of the higher excited states at large inter-nuclear distances. Very recently, Pashov et al. [26] have studied the $1\ ^1\Pi$ (B) and Grochola et al. [30] the $2\ ^1\Pi$ (D) excited states. They founds potential well depth of 1686 cm^{-1} and 1664.3 cm^{-1} respectively for the B and D states, located at an equilibrium distance of 6.979 a.u. and 7.60 a.u. Our equilibrium distances are in good agreement with these data, while D_e values are somewhat underestimated as in the previous theoretical study [18]. Our term energies values T_e for the $1\ ^1\Pi$ (B) and $2\ ^1\Pi$ (D) states are overestimated compared to the experimental ones [26,30,31] (see Table 6). However, it is not clear if zero point energy corrections are needed or not. The present values are taken from the bottom of the ground state well. If we made the correction, then the agreement improves considerably.

As can be seen in Table 6, for the highly excited states also, our results for the main spectroscopic constants are in good agreement with the recent experimental data [32]. We find, for example, for the 6 and 7 $^1\Pi$ states, equilibrium distances R_e = 7.18 a.u. and R_e = 7.42 a.u., respectively, and wells depths, D_e = 4191 cm^{-1} and D_e = 4023 cm^{-1}, compared with the experimental data of Jedrzejewski-Szmek et al. [32], R_e = 7.352 a.u., 7.415 a.u. and D_e = 4219 cm^{-1} and 4012 cm^{-1}, respectively.

Table 6
Spectroscopic constants R_e (in a.u.), D_e (in cm^{-1}), ω_e (in cm^{-1}) and T_e (in cm^{-1}) of the $^1\Pi$ states of LiK molecule compared with the available results in the literature.

State	R_e	D_e	ω_e	T_e	Ref.
$1^1\Pi$	7.19	1454	122.97	17,672	This work
	7.00				Exp. [25]
	6.979	1686	135.8370	17572.760	Exp. [26]
	7.06	1517	131.00	17,725	Theory [18]
$2^1\Pi$	7.69	1300	120.92	20,410	This work
	7.60	1664.3	128.978	19455.73	Exp. [30]
	7.56			21120.05	Exp. [31]
	7.56	1584	132.30	19,541	Theory [18]
$3^1\Pi$	7.29	1584	92.53	26,029	This work
	8.05	1624	102.35	26,131	Theory [18]
$4^1\Pi$	7.28	4144	137.93	26,595	This work
$5^1\Pi$	7.45	5011	114.13	28,427	This work
$6^1\Pi$	7.18	4191	134.75	29,843	This work
	7.352	4219		29886.28	Exp. [32]
$7^1\Pi$	7.42	4023	160.25	29,961	This work
	7.415	4012		30093.51	Exp. [32]
$8^1\Pi$	7.15	3672	58.62	30,475	This work
$1^3\Pi$	6.09	8504	204.57	10,534	This work
	6.06	8767	208.39	10,475	Theory [18]
$2^3\Pi$	7.58	612.49	123.60	21,090	This work
	7.56	736	108.90	20,388	Theory [18]
$3^3\Pi$	9.85	3283	83.74	26,652	This work
	9.84	3384	82.40	24,373	Theory [18]
$4^3\Pi$	7.63	4627	200.69	27,870	This work
$5^3\Pi$	7.69	5265	114.66	29,591	This work
$6^3\Pi$	6.40	4915	162.27	29,878	This work
$7^3\Pi$	8.66	3504	152.63	31,019	This work
$8^3\Pi$	7.42	3949	127.56	31,458	This work

Table 7
Spectroscopic constants R_e (in a.u.). D_e (in cm^{-1}), ω_e (in cm^{-1}) and T_e (in cm^{-1}) of the $^{1,3}\Delta$ states of LiK molecule compared with the available results in the literature.

State	R_e	D_e	ω_e	T_e	Ref.
$1^1\Delta$	6.78	4026	156.70	23,515	This work
	6.66	4230	161.00	23,525	Theory [18]
$2^1\Delta$	7.30	4310	145.25	29,097	This work
	6.86	4800	157.10	28,837	Theory [18]
$3^1\Delta$	7.03	5354	148.64	27,604	This work
$4^1\Delta$	7.26	5002	161.00	29,146	Theory [18]
	7.29	4487	149.48	31,744	This work
	7.06	2714	156.20	31,433	Theory [18]
$1^3\Delta$	7.03	3124	187.55	24,418	This work
	7.06	3278	156.20	24,478	Theory [18]
$2^3\Delta$	7.31	4340	197.21	29,066	This work
	7.26	4521	145.73	29,116	Theory [18]
$3^3\Delta$	7.17	4561	139.93	30,691	This work
	7.16	4477	156.8	29,670	Theory [18]
$3^3\Delta$	7.30	4534	338.33	31,684	This work
2nd min	17.19	622			

3.2. Diabatic results

In our study, a set of 12 adiabatic states at the largest distance (400 a.u.) are taken as references (the 11 lowest in energy and the ionic state). At this distance, diabatic and adiabatic states coincide

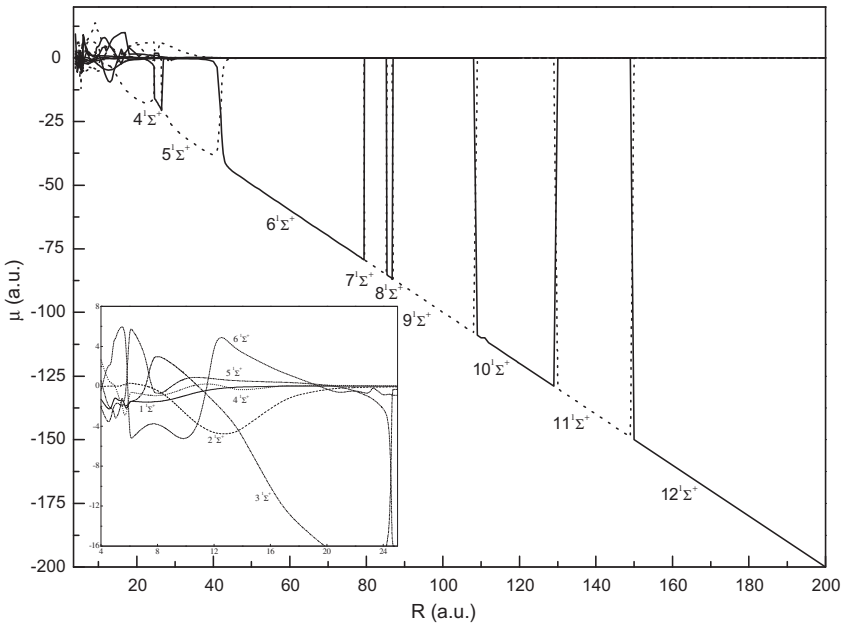

Fig. 9. Adiabatic permanent dipole moments μ for the 4–12 $^1\Sigma^+$states of the LiK molecule, as a function of the inter-nuclear distance R.

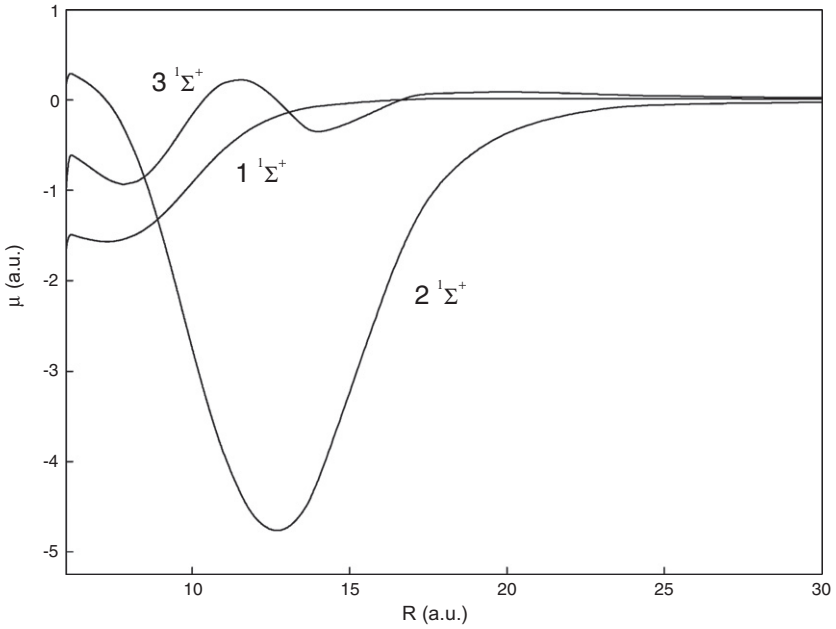

Fig. 10. Adiabatic permanent dipoles moments for the 1–3 $^1\Sigma^+$ states of the LiK molecule, as a function of the inter-nuclear distance R.

and the ionic state can be easily identified while all neutral ones have reached their asymptotic limits. We present the resulting 12 $^1\Sigma^+$ diabatic potential energy curves in Fig. 6 where they are labeled D_1 for the ionic Li^-K^+ and D_2 to D_{12} for other. We clearly observed that D_1, the ionic state, crosses all other states D_{2-12} at different distances. The lowest crossings in energy occurs with D_2 (Li(2s)K(4s)) around 10.6 a.u., D_3 (Li(2s)K(4p)) around 14.9 a.u. and with D_4 (Li(2p)K(4s)) around 15.5 a.u. The other crossings occur at much larger distances and higher energies. The actual crossings in the diabatic representation are transformed into avoided crossings in the adiabatic picture. In the adiabatic representation, see Fig. 1, the ionic branches are spread into various adiabatic states. Inspection of the magnitude of coupling supports the conclusion that the coupling decreases with increasing distances, and therefore the avoided neutral-ionic crossings becomes less and less avoided as the underlying ionic state encounters high energy Rydberg flat at larger internuclear distances.

4. Adiabatic and diabatic permanent and transition electric dipole moments

4.1. Permanent dipole moment

The permanent dipole moments are illustrated in Figs. 9 and 10 ($^1\Sigma^+$) and in Fig. 12 ($^3\Sigma^+$) for the adiabatic states and in Fig. 11

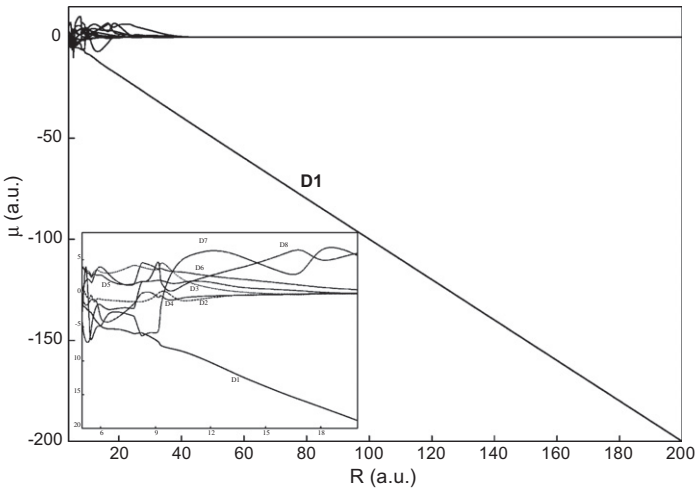

Fig. 11. Diabatics permanent dipole moment for the first 12 $^1\Sigma^+$ states of the LiK, as a function of the inter-nuclear distance R.

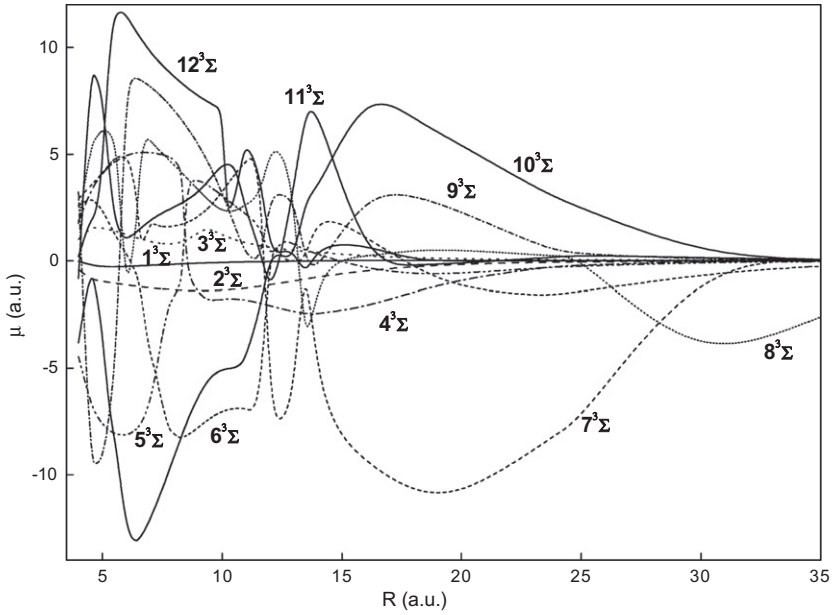

Fig. 12. Adiabatic permanent dipoles moment for the $12^3\Sigma^+$ states of LiK.

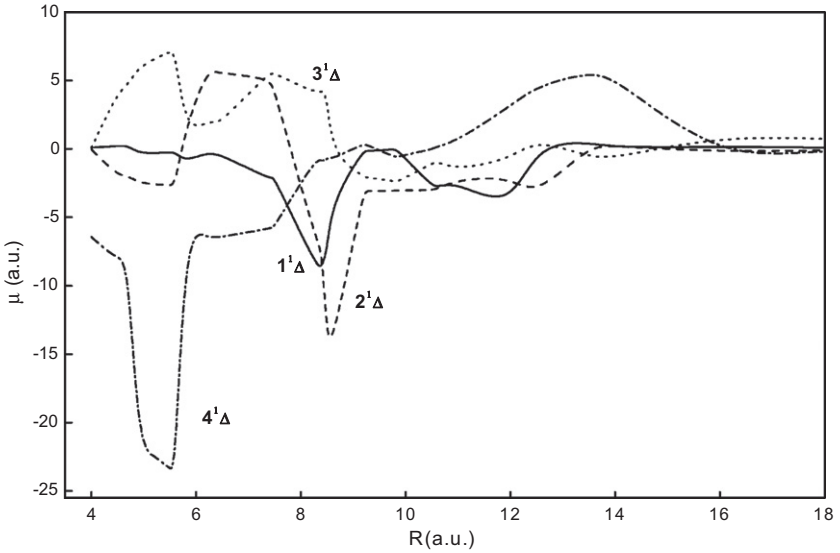

Fig. 13. Adiabatic permanent dipole moment of the first four $^1\Delta$ states of LiK.

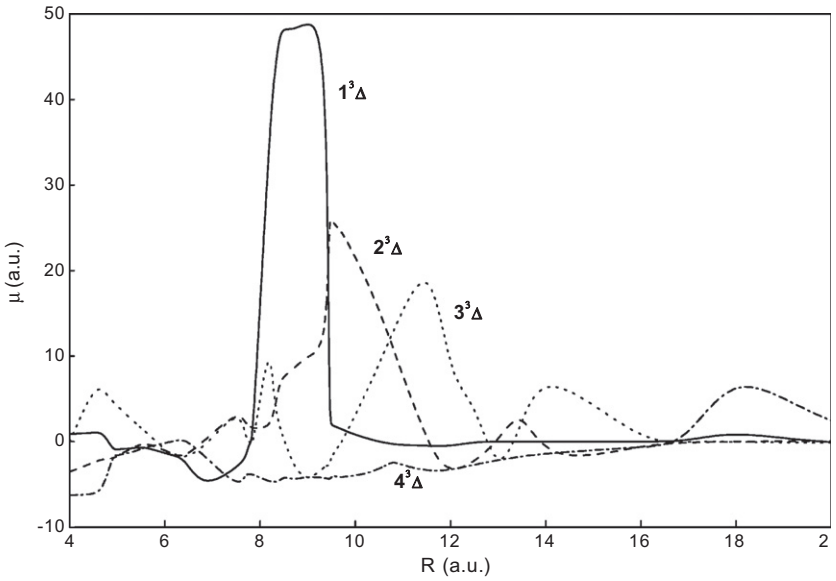

Fig. 14. Adiabatic permanent dipole moment of the first four $^3\Delta$ states of LiK.

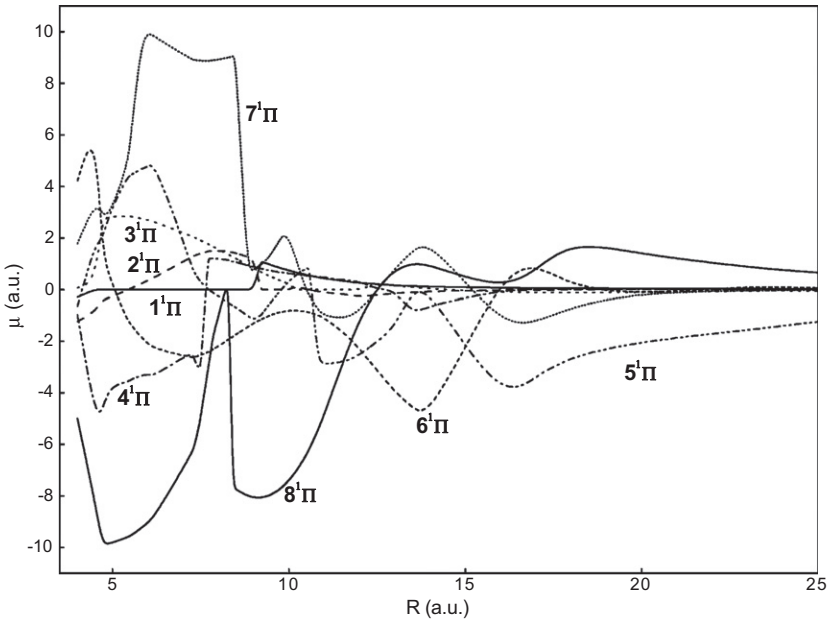

Fig. 15. Adiabatic permanents dipoles moment of the 8 $^1\Pi$ states of LiK.

($^1\Sigma^+$) for the diabatic states. We considered a large range of inter-nuclear distances because we expected interesting features to arise from a global picture also involving the highly excited states, which become ionic at large inter-nuclear distances. Let us consider the diabatic results. This is the first direct *ab initio* evaluation of the dipole moment for the diabatic states of KLi.

The variation of permanent dipoles present a specific character for ionic diabatic state where a linear dependence is expected. While the permanent dipole of the neutral diabatic should vanish at large distance. This is the behavior observed in Fig. 11, the permanent dipole moment of D_1 behaves as $-R$, except at very short distances, and those of the neutral states drop to zero as the distance increases. This behavior corresponding to the physically expected one gives support to the diabatization method used. For the adiabatic representation, for the permanent dipole moment, we observe that one after another, each state goes to a maximum and then falls to zero. Altogether they reproduce piecewise the linear behavior of the ionic state. Moreover, the crossings between successive branches can be related to the neutral-ionic avoided crossings between the adiabatic potential curves. A similar behavior has been observed for the alkali hydride series [36–39,41]. The permanent dipole gives actually a direct illustration of the ionic character of the adiabatic electronic wave function. We thus access directly a visualization of the *R*-dependence of the charge distribution of the wave function. The distance for which two consecutive adiabatic states have the same dipole locates the crossing of the ionic diabatic state with the corresponding neutral one. The sharpness of the slopes around the node for the dipole is closely related to the weakness of the avoided crossing for the energy.

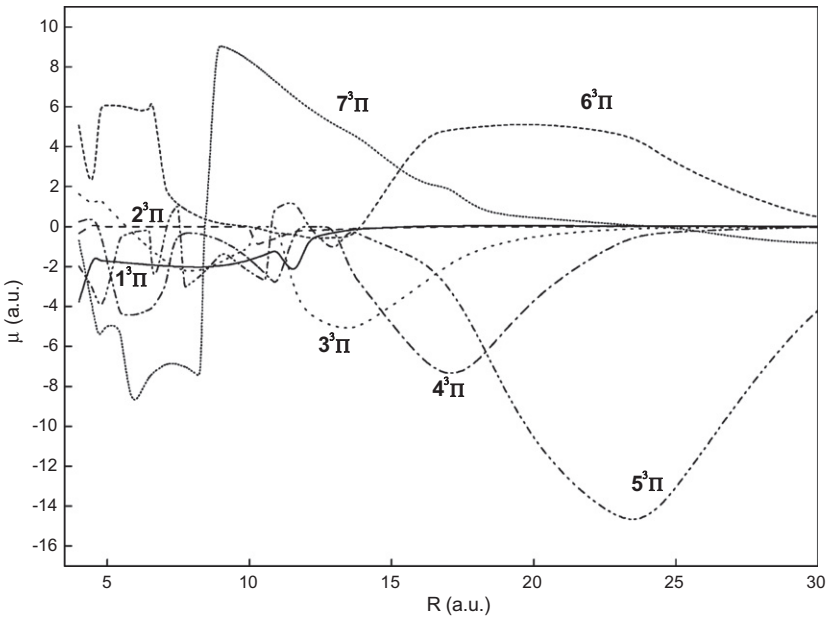

Fig. 16. Adiabatic permanents dipoles moment of the 8 $^3\Pi$ states of LiK.

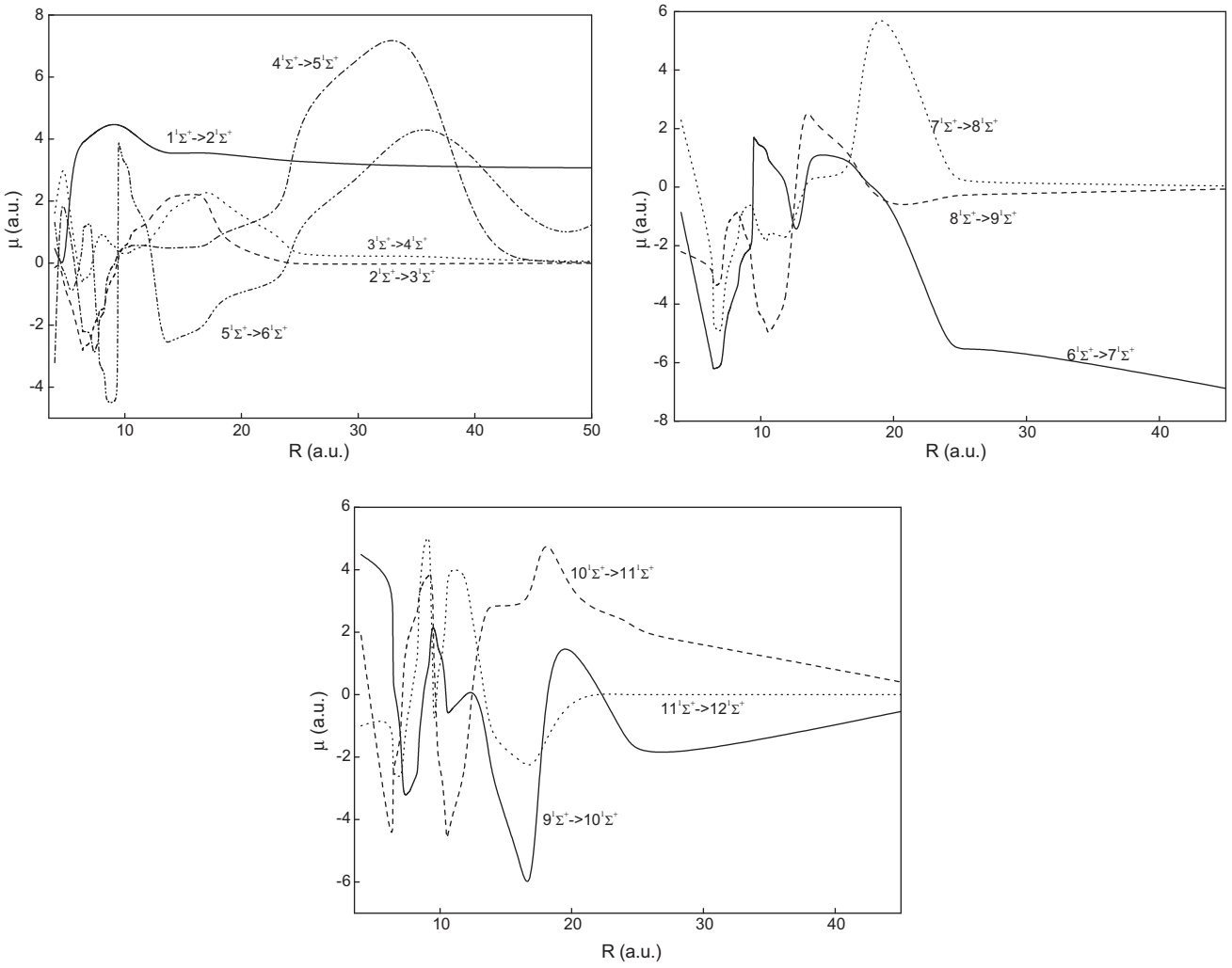

Fig. 17. Transition dipole moment between neighboring states of $^1\Sigma^+$ symmetry.

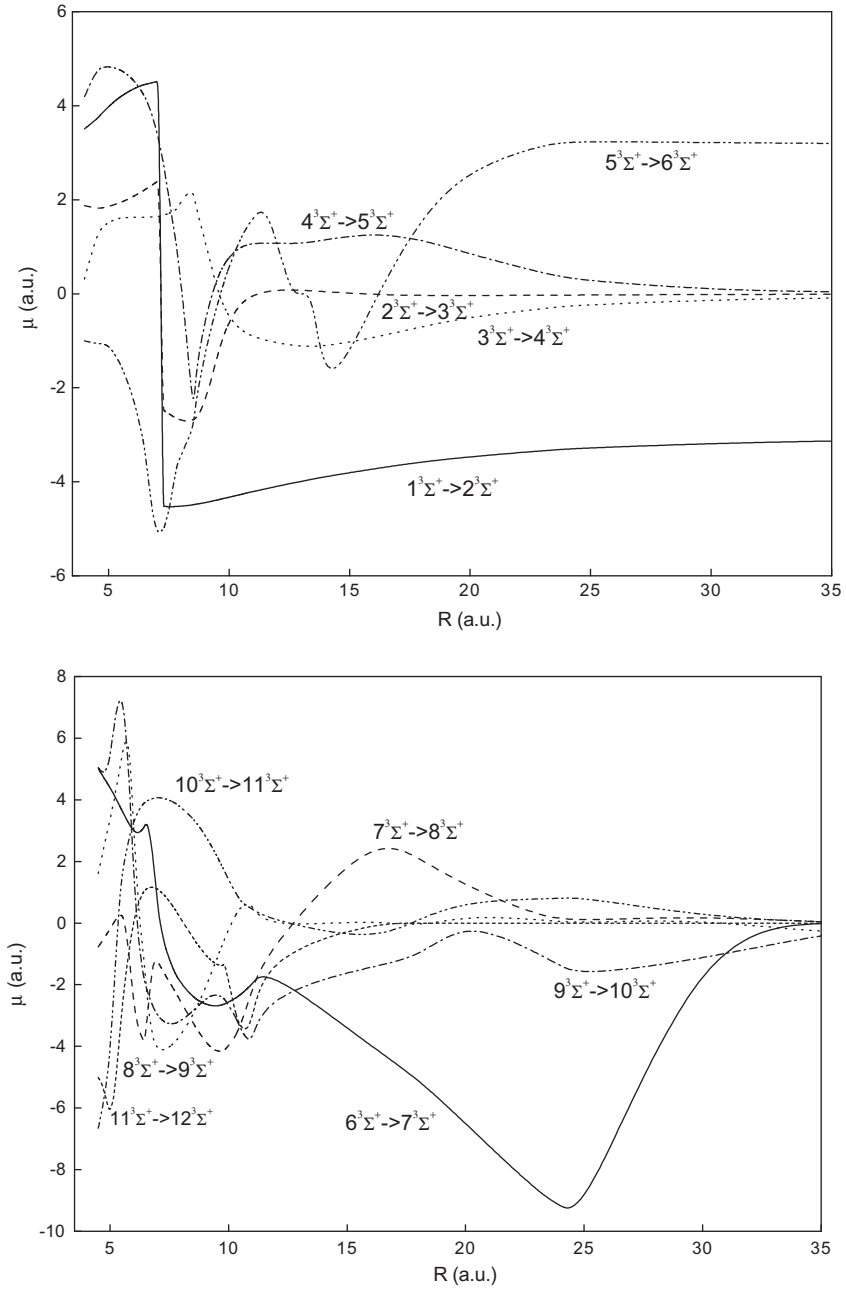

Fig. 18. Transition dipole moment between neighboring states of $^3\Sigma^+$ symmetry.

The permanent dipole moment has been also determined for the electronic states of the $^3\Sigma^+$, $^1\Pi$, $^3\Pi$, $^1\Delta$, and $^3\Delta$ symmetries. Their permanent dipole moments are displayed in Figs. 12–16. They are not negligible and become particularly significant for higher excited states. At large distance they decrease and vanish. They present strong variations but only some of them can be related to avoid crossings.

4.2. Transition dipole moments

It is also interesting to illustrate the behavior of the transition dipole moments. We have selected a few ones $^1\Sigma^+$ symmetry, reported in Fig. 17, $^3\Sigma^+$, Fig. 18, $^1\Pi$, Fig. 19, $^3\Pi$, Fig. 20, $^{1,3}\Delta$, Fig. 21. Strong variations are clearly present. Again, the avoided crossings between the potential curves illustrate changes in the electronic wave functions and found some reflect here. However, these crossings cannot easily explain all the variations. For example, the avoided crossing between the states $^1\Sigma^+$ 7 and 8 just below 20 a.u. generate a peak in the corresponding transition dipole moment (top of second figure in Fig. 20) illustrating the exchange in their physical electronic characteristics. The transition moments reaching a non-zero asymptotic value, obviously correspond to allowed atomic transitions. For the 3Sigma, the transition dipole moments are rather involved too, as well as for the other symmetries, although smoother behavior where naively expected.

5. Conclusion

In this paper, we have performed an *ab initio* study for 48 electronic states of the LiK molecule dissociating into K (4s, 4p, 4d, 5s, 5p, 5d, 6s) + Li (2s, 2p, 3s). The calculation method used in our study is based on a non-empirical pseudo-potential approach for

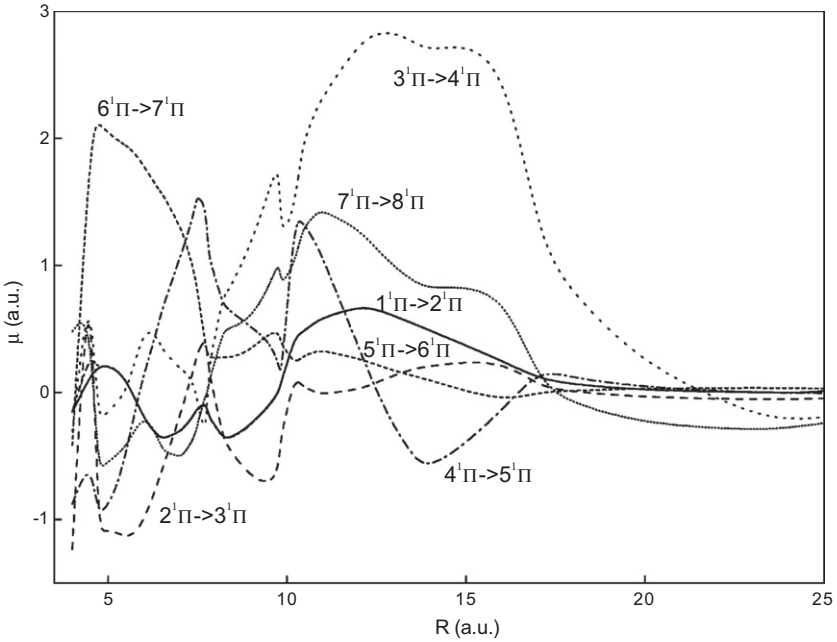

Fig. 19. Transition dipole moment between neighboring states of $^1\Pi$ symmetry.

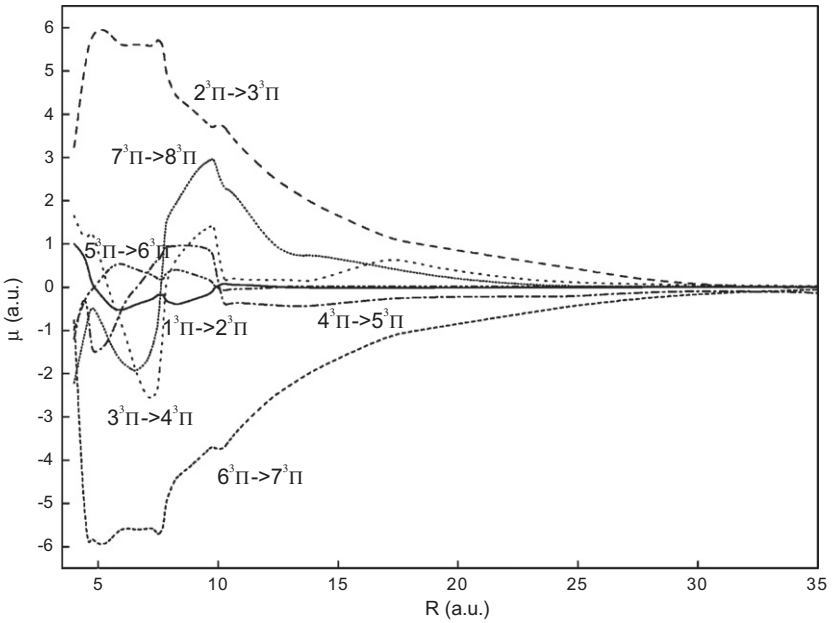

Fig. 20. Transition dipole moment between neighboring states of $^3\Pi$ symmetry.

the Li and K cores complemented by operatorial Core Polarization Potentials which allow taking into account the core valence correlation effects. The adiabatic potential energy curves and permanent and transition dipole moments have been computed for a large and dense grid of inter-nuclear distances. The spectroscopic constants of the 1–12 $^{1,3}\Sigma^+$, 1–8 $^{1,3}\Pi$, and 1–4 $^{1,3}\Delta$ electronic states have been extracted and compared with the available theoretical [23,18] and experimental works [24–32]. The agreement between the experimental spectroscopic constants and the ones obtained in our study for the ground and first excited states was shown to be good. Moreover, the comparison with the IPA potential for the 4 $^1\Sigma^+$, shows an excellent agreement despite of the rather unusual shape of this potential.

A diabatization is performed for the first time to the LiK molecule in order to determine the $^1\Sigma^+$ diabatic states. The imprint of the ionic states Li^-K^+ is thus clearly illustrated. The diabatic Li^-K^+ curve is observed to cross almost all neutral states, leading in $^1\Sigma^+$ symmetry to series of avoiding crossings located at short, intermediate, and large distances. These results can be easily understood from the physical nature of the diabatic states and they shed light on the interplay between the ionic and neutral species that dominate the alkali dimers potential curves. Such crossings became avoided crossings in the adiabatic scheme and produce undulating behaviors for several adiabatic states. These diabatic data could be used to determine accurate positions and non-radiative lifetimes of the vibrational levels, including nonadiabatic effects.

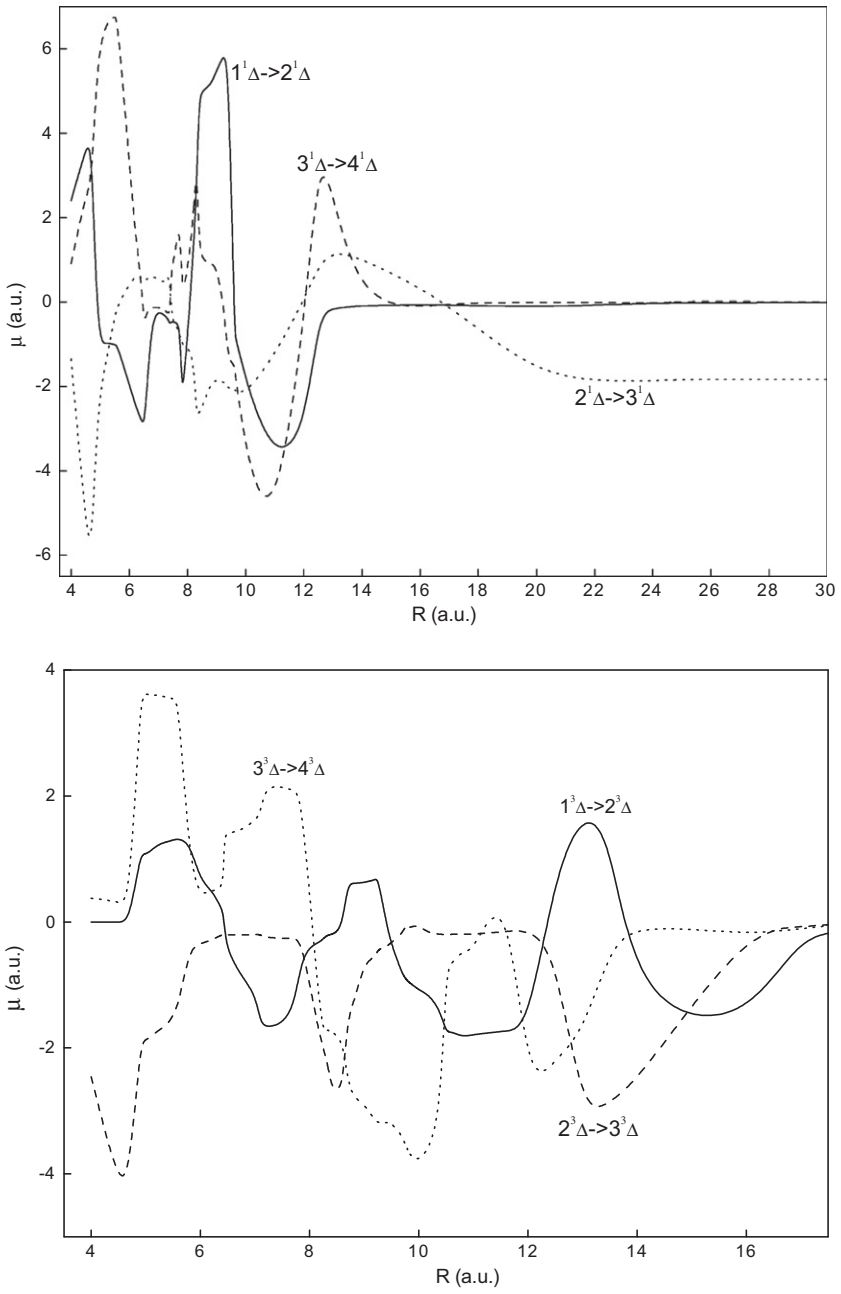

Fig. 21. Transition dipole moment between neighboring states of $^1\Delta$ and $^3\Delta$ symmetries.

Acknowledgments

The authors wish to thank the anonymous referees for their careful reading of the manuscript and their fruitful comments and suggestions.

Appendix A. Supplementary material

Supplementary data associated with this article can be found, in the online version, at doi:10.1016/j.chemphys.2011.07.010.

References

[1] I.W.M. Smith, Low Temperatures and Cold Molecules, Imperial College Press, 2008.
[2] R.V. Krems, W.C. Stwalley, B. Friedrich, Cold Molecules, Theory, Experiment, Applications, CRC Press, 2009.
[3] O. Dulieu, C. Gabbanini, Rep. Prog. Phys. 72 (2009) 086401.
[4] L.D. Carr, J. Ye, New J. Phys. 11 (2009) 055009.
[5] A.N. Nikolov, E.E. Eyler, X.T. Wang, J. Li, H. Wang, W.C. Stwalley, P.L. Gould, Phys. Rev. Lett. 82 (1999) 703.
[6] J. Deiglmayr, A. Grochola, M. Repp, K. Mortlbauer, C. Glück, J. Lange, O. Dulieu, R. Wester, M. Weidemüller, Phys. Rev. Lett. 101 (2008) 133004.
[7] M. Viteau, A. Chotia, M. Allegrini, N. Bouloufa, O. Dulieu, D. Comparat, P. Pillet, Science 321 (2008) 232.
[8] M. Viteau, A. Chotia, M. Allegrini, N. Bouloufa, O. Dulieu, D. Comparat, P. Pillet, Phys. Rev. A 79 (2009) 021402.
[9] D. Sofikitis, S. Weber, A. Fioretti, R. Horchani, M. Allegrini, B. Chatel, D. Comparat, P. Pillet, New J. Phys. 11 (2009) 055037.
[10] K.-K. Ni, S. Ospelkaus, M.H.G. de Miranda, A. Peer, B. Neyenhuis, J.J. Zirbel, S. Kotochigova, P.S. Julienne, D.S. Jin, J. Ye, Science 322 (2008) 231.
[11] J.G. Danzl, M.J. Mark, E. Haller, M. Gustavsson, N. Bouloufa, O. Dulieu, H. Ritsch, R. Hart, H.-C. Nägerl, Faraday Discuss. 142 (2009) 1.
[12] D. Pavolini, T. Gustavsson, F. Spigelmann, J.P. Daudey, J. Phys. B: Atom. Mol. Opt. Phys. 22 (1989) 1721.

[13] A.R. Allouche, M. Korek, K. Fakherddin, A. Chalaan, M. Dagher, F. Taher, M.J. Aubert-Fecon, Phys. B: Atom. Mol. Opt. Phys. 33 (2000) 2307.
[14] H. Fahs, A.R. Allouche, M. Korek, J. Phys. B 35 (2002) 1501.
[15] M. Korek, A.R. Allouche, M. Kobeissi, A. Chaalan, M. Dagher, F. Fakherddin, M. Aubert-Frecon, Chem. Phys. 256 (2000) 1.
[16] M. Korek, A.R. Allouche, K. Fakhreddine, A. Chaalan, Can. J. Phys. 78 (2000) 977.
[17] S. Rousseau, A.R. Allouche, M. Aubert-Frécon, J. Mol. Spectrosc. 203 (2000) 235.
[18] S. Rousseau, A.R. Allouche, M. Aubert-Frécon, S. Magnier, P. Kowalczyk, W. Jastrzebski, Chem. Phys. 247 (1999) 193.
[19] S. Magnier, M. Aubert-Frécon, P. Millié, J. Mol. Spectrosc. 200 (2000) 96.
[20] S. Magnier, M. Aubert-Frécon, P. Millié, Phys. Rev. A 54 (1996) 204.
[21] I. Schmidt-Mink, M. Müller, W. Meyer, Chem. Phys. Lett. 112 (1984) 120.
[22] I.D. Petsalakis, D. Tzeli, G. Theodorakopoulos, J. Chem. Phys. 129 (2008) 054306.
[23] W. Muller, W. Meyer, J. Chem. Phys. 80 (1984) 3311.
[24] V. Bednarska, I. Jackowska, W. Jastrzebski, P. Kowalczyk, J. Mol. Spectrosc. 189 (1998) 244.
[25] V. Bednarska, P. Kowalczyk, W. Jastrzebski, J. Mol. Spectrosc. 180 (1996) 435.
[26] A. Pashov, W. Jastrzebski, P. Kowalczyk, Chem. Phys. Lett. 292 (1998) 615.
[27] A. Grochola, P. Kowalczyk, W. Jastrzbski, P. Crozet, A.J. Ross acta, Phys. Pol. A 102 (2002).
[28] J. Szczepkowski, A. Grochola, W. Jastrzebski, P. Kowalczyk, Chem. Phys. Lett. 499 (2010) 36.
[29] H. Salami, A.J. Ross, P. Crozet, W. Jastrzebski, P. Kowalczyk, R.J. Le Roy, J. Chem. Phys. 126 (2007) 194313.
[30] A. Grochola, W. Jastrzebski, P. Kowalczyk, P. Crozet, A.J. Ross, Chem. Phys. Lett. 372 (2003) 173.
[31] W. Jastrzebski, P. Kowalczyk, A. Pashov, J. Szczepkowski, Spectrochim. Acta Part A 73 (2009) 117.
[32] Z. Jedrzejewski-Szmek, D. Łubinski, P. Kowalczyk, W. Jastrzebski, Chem. Phys. Lett. 458 (2008) 64.
[33] W. Muller, J. Flesh, W. Meyer, J. Chem. Phys. 80 (1984) 3297.
[34] J.C. Barthelat, Ph. Durand, A. Serafini, Mol. Phys. 33 (1975) 179.
[35] J.C. Barthelat, Ph. Durand, Gazz. Chim. Ital. 108 (1978) 255.
[36] N. Khelifi, B. Oujia, F.X. Gadea, J. Chem. Phys. 116 (2002) 2879.
[37] N. Khelifi, W. ZRafi, B. Oujia, F.X. Gadea, Phys. Rev. A 65 (2002) 042513.
[38] W. Zrafi, N. Khelifi, B. Oujia, F.X. Gadea, J. Phys. B: Atom. Mol. Opt. Phys. 39 (2006) 3815.
[39] Neji Khelifi, J. Russ. Laser Res. 29 (2008) 274.
[40] M. Foucrault, Ph. Millie, J.P. Daudey, J. Chem. Phys. 96 (1992) 1257.
[41] A. Boutalib, F.X. Gadea, J. Chem. Phys. 97 (1992) 1144.
[42] F.X. Gadea, thèse d'état, Université Paul Sabatier, Toulouse, 1987.
[43] F.X. Gadea, M. Pelissier, J. Chem. Phys. 93 (1990) 545.
[44] T. Romero, A. Aguilar, F.X. Gadea, J. Chem. Phys. 110 (1999) 6219.
[45] F.X. Gadea, Phys. Rev. A 43 (1991) 1160.
[46] R. Hoffmann, J. Chem. Phys. 39 (1963) 397.
[47] C.E. Moore, Natl. Bur. Stand. Circ., U.S GPO, Washington, DC, 1971, No. 467.